UNIVERSIDADE ESTADUAL DE CAMPINAS
SISTEMA DE BIBLIOTECAS DA UNICAMP
REPOSITÓRIO DA PRODUÇÃO CIENTIFICA E INTELECTUAL DA UNICAMP

Versão do arquivo anexado / Version of attached file:

Versão do Editor / Published Version

Mais informações no site da editora / Further information on publisher's website:

https://journals.aps.org/prb/abstract/10.1103/PhysRevB.74.075319

DOI: 10.1103/PhysRevB.075319

Direitos autorais / Publisher's copyright statement:

Hafnium silicide formation on Si(100) upon annealing

A. de Siervo,[1,2,][*] C. R. Flüchter,[1] D. Weier,[1] M. Schürmann,[1] S. Dreiner,[1] C. Westphal,[1] M. F. Carazzolle,[3] A. Pancotti,[3]
R. Landers,[3] and G. G. Kleiman[3]

[1]*Experimentelle Physik 1, Universität Dortmund, Otto-Hahn-Str. 4, D 44221 Dortmund, Germany*
[2]*Laboratório Nacional de Luz Síncrotron, Caixa Postal 6192, 13084-971, Campinas, São Paulo, Brazil*
[3]*Instituto de Física "Gleb Wataghin," Universidade Estadual de Campinas, Caixa Postal 6165, 13083-970, Campinas,*
São Paulo, Brazil

High dielectric constant materials, such as HfO_2, have been extensively studied as alternatives to SiO_2 in new generations of Si based devices. Hf silicate/silicide formation has been reported in almost all literature studies of Hf based oxides on Si, using different methods of preparation. A silicate interface resembles close to the traditional Si/SiO_2. The silicate very likely forms a very sharp interface between the Si substrate and the metal oxide, and would be suitable for device applications. However, the thermal instability of the interfacial silicate/oxide film leads to silicidation, causing a dramatic loss of the gate oxide integrity. Despite the importance of the Hf silicide surface and interface with Si, only a few studies of this surface are present in the literature, and a structural determination of the surface has not been reported. This paper reports a study of the Hf silicide formation upon annealing by using a combination of XPS, LEED, and x-ray photoelectron diffraction (XPD) analyses. Our results clearly indicate the formation of a unique ordered Hf silicide phase ($HfSi_2$), which starts to crystallize when the annealing temperature is higher than 550 °C.

PACS number(s): 81.05.Je, 79.60.Dp, 61.14.Qp, 61.14.Hg

I. INTRODUCTION

Over more than five decades the rate and scale of miniaturization of integrated circuit elements followed Moore's Law.[1] Today it is facing its limits. Up to now, almost all semiconductor devices are based on Si/SiO_2 technology, where the SiO_2 dielectric compound allowed a continuous development of the technology which made the production of semiconductor devices easy, efficient, and cheap. However, miniaturization of the devices has made the SiO_2 dielectric so thin that the resulting leakage current due to electron tunneling and charge trapping at the interfaces becomes unacceptable for the new low power and high frequency devices.[2] Therefore, there has been a great deal of effort to find a substitute for the SiO_2 dielectric.[3] The basic idea is to find a material with a higher dielectric constant (k) than that of SiO_2, but compatible with the present Si technology. Such a "*high-k*" material would allow the miniaturized device to perform adequately by increasing the physical thickness of the gate dielectric (for a given capacitance), and by dramatically reducing the tunneling current. Such a candidate material should be compatible with Si electronically and structurally to produce the same favorable properties as the SiO_2. In particular, the interface should be thermally stable against degradation. Candidates such as CeO_2, Y_2O_3, and Al_2O_3 are not very attractive as substitutes because of their relative low dielectric constants compared to those of SiO_2 or Si_3N_4, which are already used. Some ultrahigh-k materials may cause poor short channel effects due to the fringing field induced barrier lowering effect.[4] For many promising *high-k* materials such as Ta_2O_5 and TiO_2 it is known that they are thermally unstable and a silicidation process occurs in the oxide/Si interface and forms a low-k interfacial layer.[5]

In the past three to five years, a great deal of attention has been focused on hafnium oxide because of its relatively high dielectric constant of 20-25, and because of its wide band gap of 5.7–5.8 eV. Further, hafnium oxide has a high thermal stability as a bulk material. However, as in the cases of the other SiO_2 substitute candidates, the formation of metallic Hf or Hf silicide components during the annealing process raises a serious problem, which must to be solved. Some results in the literature indicate that it may be possible to stabilize the interface with Si and maintain the desirable electronic and structural properties of a sharp Hf silicate interface between the Si and HfO_x film.[3]

Recent results indicate that the thermal stability seems to be strongly dependent on the presurface created on the Si before the HfO_x deposition and on the subsequent annealing procedure.[6–9] However, almost all of the published results indicate[5,14,19] that a high temperature annealing produces an inevitable Hf silicide component, which starts to form at the interface.

The new generation of electronic devices presents the challenge to design gate dielectrics with almost atomic dimensions. Their production requires new preparation methods and a better understanding of the electronic and geometric structure on an atomic scale as well. Despite the importance of a better understanding of these issues, their surface, interface, and even the bulk structure of the Hf/Si system are poorly known. In the case of Hf silicide on Si(100) an unequivocal determination of the surface and interface structure represents a necessary ingredient to find a recipe to thermally stabilize the surface. Up to now there are no reports of structure surface determination neither of the Hf silicide nor HfO_x films.

In this paper, we present a systematic and multitechnique study of the Hf silicidation process, when ultrathin or thin films (0.3 nm to 3 nm) of metallic Hf grown on Si(100) are annealed at different temperatures in the range of 300 to 1000 °C. One important question that we address is

related to the structural phase formed by the Hf silicide on Si(100). Some results in the literature claim the possibility of a phase transition from HfSi to $HfSi_2$ (Refs. 11–13) depending on the annealing process. In order to clarify this question, we applied x-ray photoelectron spectroscopy (XPS), angle-scanned photoelectron diffraction (XPD), low-energy electron diffraction (LEED), and a comprehensive XPD theory-experiment analysis. Our results, mainly supported by the XPD theory-experiment analysis, indicate that only one ordered phase, the $HfSi_2$, seems to be formed when metallic Hf is evaporated on the clean Si(100) surface with a subsequent annealing process. In this paper we present the first XPD study of hafnium silicide and we compare the experimental diffraction patterns with the results from simulations for model structures.

II. EXPERIMENT

The experiment was performed in a μ-metal UHV chamber with a based pressure below 1.0×10^{-10} mbar, equipped with a high resolution electron analyzer, LEED optics, *e*-beam evaporators, and a high precision sample manipulator specially designed for angle-scanned photoelectron diffraction experiments. The manipulator and the sample holder were designed to allow sample transfer and resistive heating up to 1200 °C. A commercial Si(100) single crystal (0.5 mm thick, *p* doped), previously cleaned with isopropanol, was mounted into the sample holder with Mo plates as electrical contacts, and a 6 mm diameter sample area was kept free. The sample and the sample holder were thoroughly degassed in UHV before removing the natural SiO_2 layer in order to prevent contamination of the sample surface by such gases as H_2O, N_2, and CO. During the degassing process, the pressure was always lower than 1.0×10^{-8} mbar. The natural SiO_2 layer was removed by flash heating the sample at temperatures up to 1000 °C. The temperature was monitored by an infrared pyrometer. During the flash heating, the pressure was kept below 5.0×10^{-10} mbar. By means of a high temperature *e*-beam evaporator, metallic Hf from a previously degassed Hf wire was deposited on the clean Si(100)-(2 $\times$1)2D reconstructed surface. The 2D notation means that the surface is reconstructed in two domains rotated by 90°. During the Hf deposition, the pressure was kept lower than 4.0×10^{-10} mbar. Contaminants such as C, N, and O were below the detection limit of XPS. The film was homogeneously distributed over the surface as could be verified by XPS measurements taken on different regions of the sample. The ratio between Si 2*p* and Hf 4*f* was the same over the surface with variation less than 5%. The thickness was correlated to the Hf and Si XPS signals by assuming a near layer-by-layer growth mode, and the corresponding Si and Hf inelastic mean free paths were determined from the Tanuma-Powell-Penn formula.[16] In Fig. 1(a), we display the XPS results for clean Si and for an equivalent 3 nm Hf film as evaporated and measured in normal emission, as well as the calibration curve for the Hf film thickness, in Fig. 1(b). The equivalent Hf thickness displayed in Fig. 1(b) and from now referenced in the text means the amount of Hf necessary to exponentially attenuate the XPS Si 2*p* intensity by the
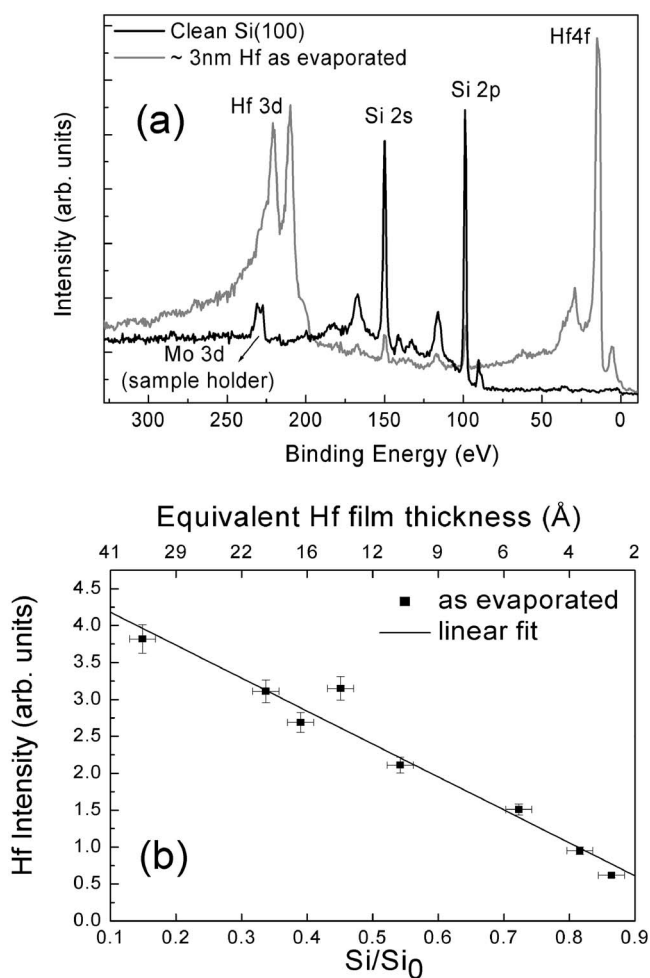

FIG. 1. (a) XPS scans excited with Mg $K\alpha$ of the clean Si(100) (black curve) and approximately 3 nm of Hf as evaporated on Si(100) (gray curve). (b) Calibration of the equivalent Hf film thickness as a function of the Hf 4*f* and Si 2*p* intensities measured at normal emission. Si_0 is the Si 2*p* intensity for the clean Si (100) surface.

same factor as calculated using the layer-by-layer growth mode. The kinematics of the Hf silicide formation upon annealing was systematically followed by the XPS, LEED, and XPD measurements.

III. RESULTS

A. Thin Hf films (3 nm)

An Hf film of 3 nm equivalent thickness was grown on clean Si(100) at room temperature (RT) and was heated in consecutive steps of 1 h for each annealing temperature; each stage was monitored with XPS, LEED, and XPD measurements at RT. In a preparatory investigation we found that flash annealing produced different results from gradual annealing (i.e., during 1 h). It is clear that for this system the process of reconstruction and diffusion/segregation is a relatively slow process and so depends on the sample temperature and also on the annealing time.

By following the XPS signal during the annealing process, we determined that the XPS intensity and peak position
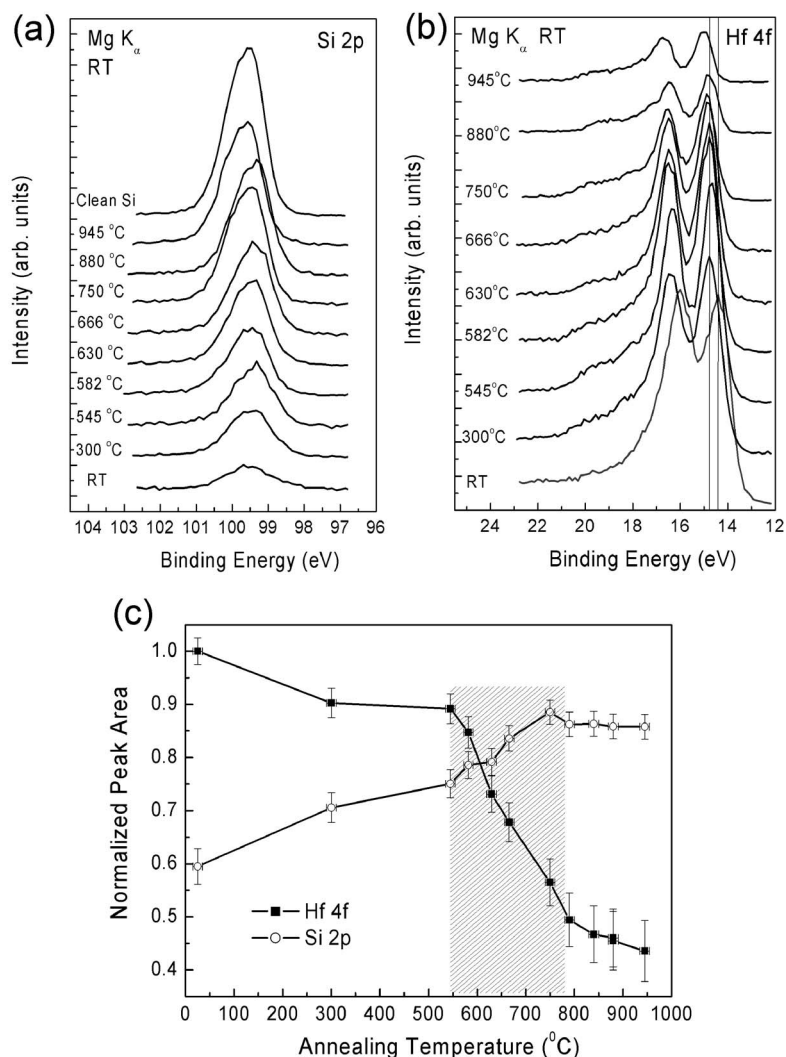
FIG. 2. High resolution XPS spectra exited with Mg $K\alpha$ and collected at normal emission for the Si $2p$ (a) and Hf $4f$ (b) of the 3 nm Hf film as functions of the exhibited consecutive annealing temperatures. (c) Normalized peak area for the Si $2p$ and Hf $4f$ as a function of the sample annealing temperature. The hatched area indicates the region of HfSi$_x$ formation.

did not change after 1 h of annealing at any specific temperature, which indicates that the sample had reached a pseudothermodynamic equilibrium in the diffusion process. We should note, however, that the peak position is very dependent on the sample temperature. This was expected for Si as a semiconductor with a temperature dependent density of states at the Fermi level. We also found that contamination could produce chemical shifts. When the samples were exposed to the normal UHV environment over long periods (typically more than 10 h), the XPS signal displayed a shift of about +0.2 eV, which is easily correlated with residual gas adsorption onto the surface (probably H or small quantities of CO). After brief heating to temperatures below 250 °C, the gas desorbed and the peak position returns to the previous value.

Figures 2(a) and 2(b) exhibit the XPS signal excited with Mg $K\alpha$ radiation for the Si $2p$ and Hf $4f$ lines, respectively; in Fig. 2(c), we present the normalized peak intensity as a function of the annealing temperature. The normalization was done dividing the intensity of the Si $2p$ and Hf $4f$ signals by the intensity of the respective clean Si $2p$ and Hf $4f$ as-evaporated. Even for the as-grown film, the Hf $4f_{7/2}$ XPS signal displays at least two components, a metallic one around 14.2 eV binding energy, and a silicide component at

around 14.6–14.8 eV, which is probably related to the interface with Si.[7,8,14] At high temperatures, starting at around 300 °C, most of the signal is converted to one narrow silicide component, which is homogeneously distributed on the surface, which corresponds to an amorphous or polycrystalline form, since LEED does not display a diffraction pattern (see Fig. 3). Increasing the annealing temperature, the XPS signal exhibits little change until we reach temperatures of around 550 °C, at which part the Hf $4f$ intensity begins to decrease markedly and the Si $2p$ intensity starts to increase strongly. As can be observed in Fig. 2(c), the decrease in the Hf $4f$ intensity is almost linear with the annealing temperature up to 800 °C, when the slope of the curve changes again.

The XPS results, by themselves, are susceptible to various explanations. The first changes in the slopes of the Hf $4f$ and Si $2p$ curves for temperatures around 550 °C are hints of the beginning of a strong Hf diffusion into the Si matrix, forming a crystalline alloy phase, which is further supported by the Hf $4f$ chemical shift to the silicide energy at around 14.6–14.8 eV binding energy. Similar results have been already reported in the literature.[7,8,14] For temperatures above 800 °C the second slope change could suggest the appearance of another phase.
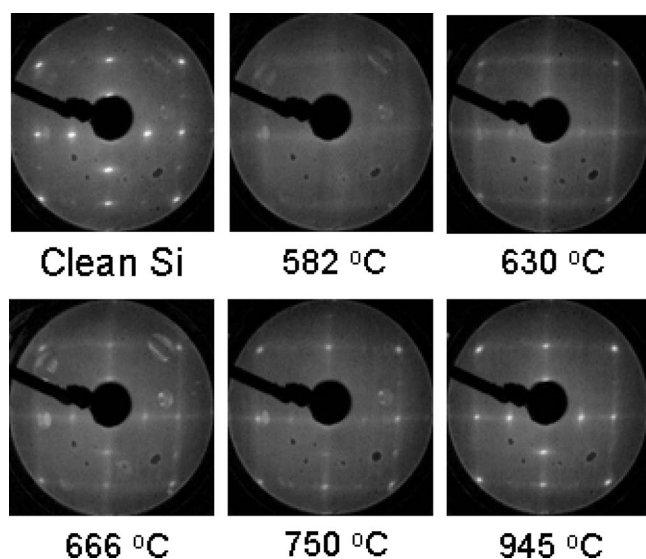
FIG. 3. LEED patterns for 100 eV primary electron energy for the 3 nm Hf film on Si(100) annealed at different temperatures.

Indeed, literature results[11–14] indicate an Hf monosilicide (HfSi) phase for the first interval of temperatures (550–800 °C) and a phase transition to Hf disilicide ($HfSi_2$) for temperatures higher than 750–800 °C. However, we should note that we observe no significant chemical shifts of the Hf $4f$ and Si $2p$ XPS spectra in the region of the second slope change, which probably indicates that no other phase forms, and that the intensity changes are related to the morphology of the surface. This interpretation is supported by AFM and STM results[14,17,18] that indicate that, in the interval from 550–800 °C, Hf diffuses through the Si, forming a $HfSi_x$ compound, and rearranging this compound on the surface,[14,17,18] for high annealing temperatures, this process is thought to find an equilibrium with a very stable Hf silicide phase that only rearranges its morphology at the surface by forming small islands,[17,18] but does not change its basic structure.

Our XPS results, however, are not sufficient in themselves to unambiguously eliminate the possibility of a phase transition or of the formation of multiple phases, since it is known from many other systems that structural phase transitions are not necessarily associated with big chemical shifts that can be observed with conventional XPS. If such phases exist, they would be associated with extra spectral components; however, the resolution of such features would require ultra-high resolution XPS spectra, which are possible to be measured at only a few synchrotron facilities.

A structural analysis is necessary to clarify whether a phase transition exists, what its details are, and what phase structure is formed at different annealing temperatures for the Hf on Si(100) system. STM is a very powerful technique, able to monitor the short and long range order on a surface, but it has no chemical sensitivity. It is most sensitive to the structure of the top layer on the surface, but structures with different chemical environments are difficult to analyze by STM only. In addition, information about the subsurface region is either not available or is accessible by STM only in a very limited manner. LEED is an important diffractive tech-

nique for solving surface structures by using the IV analysis, but it might be difficult to be useful in this particular system because of the island formation. LEED monitors long range ordered surfaces, is restricted to the first few atomic layers, and, as will be shown later in this paper, it would be very difficult to use LEED for structure determination in this particular system.

X-ray photoelectron diffraction, on the other hand, offers some advantages for the study of this particular system. Since XPD is based on photoelectron spectroscopy, it is chemically sensitive, monitors short range order and permits nondestructive depth profile analyzes by changing either the photoelectron kinetic energy or the polar angle of analysis. The existence of $HfSi_x$ on the Si(100) surface in different ordered crystalline structures as a function of the temperature, because of structural phase transitions, should be revealed in the XPD patterns.

Figure 3 exhibits the LEED patterns taken at RT for different annealing temperatures of the sample. It is clear that, for temperatures lower than 600 °C, there is no LEED pattern associated with long range order on the surface. It suggests that most of the Hf silicide formed at low annealing temperatures is present in either an amorphous or a polycrystalline phase at the surface. This is in agreement with some previous works which report that, for low temperatures, most of the $HfSi_x$ is present in an unordered phase.[9,12,14] As we raise the annealing temperature above 600 °C, a LEED pattern starts to appear, for temperatures higher than 750 °C, a clear double domain (2×1) reconstruction pattern, virtually identical to that of clean Si(100), is displayed. Such a pattern would appear to reflect the formation of large areas of clean Si(100).

Several possibilities can be adduced to explain these LEED patterns for the silicide, $HfSi_x$, for annealing temperatures between 550 and 800 °C in Fig. 3. One would be that the silicide is reconstructed, with the same unit cell as that of the Si(100)-(2×1)2D, so that the LEED pattern would be the same as that of clean Si(100) (except for possible small changes in the spot spacing associated with differences in the lattice parameter). Another possibility is that the silicide assumes a different morphology at the surface, i.e., such as islands with clean silicon surfaces between the islands. In this case, fine structures in the LEED pattern would not be clearly visible, must probably due to the lack of long range order of these islands. The LEED pattern showed for this type of situation would be the one from the clean Si surfaces between the islands. Since it is possible to see stripes and elongated points in the LEED pattern, one might think that a spot profile analysis could give information regarding the $HfSi_x$ island shape and structure.[14] In short, it is almost impossible from a conventional LEED analysis to reach definitive conclusions regarding the $HfSi_x$ surface/interface structure.

Figure 4 shows the experimental XPD patterns for the same 3 nm Hf film consecutively annealed at different temperatures. The XPD patterns are plotted in a planar projection where the intensity scale represents the anisotropy, i.e., the relative normalized area for each XPS peak of each azimuth angle by a constant background of the respective polar angle. Due the shape of the Mo clamps which hold the
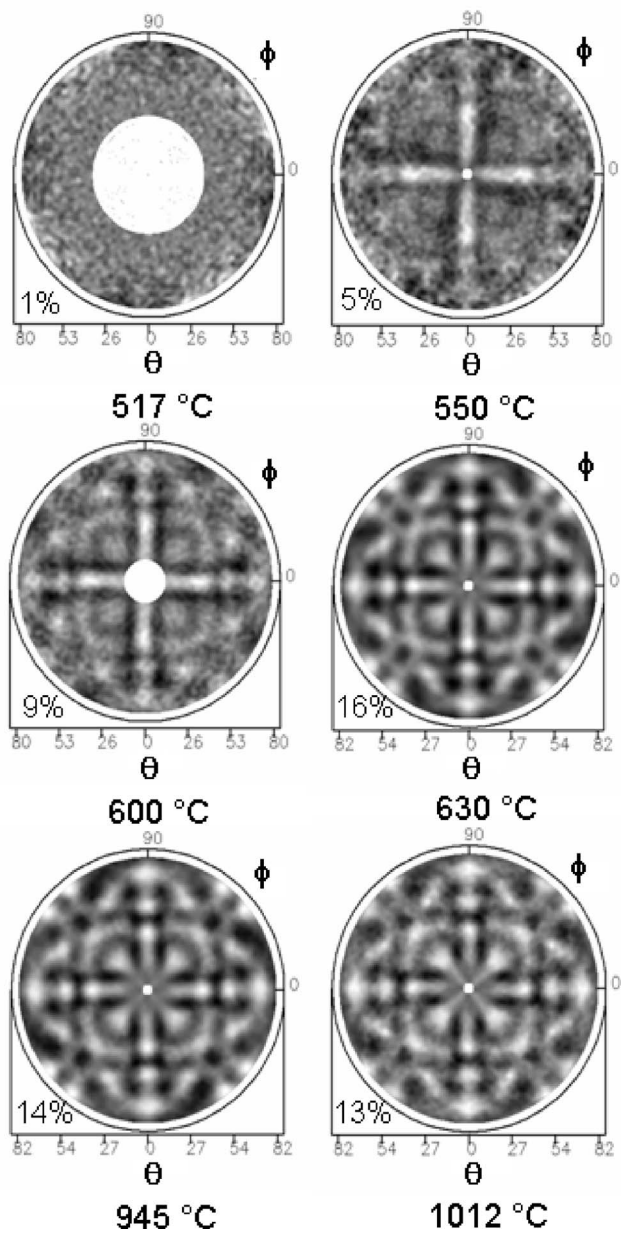
Hf 4f signal of 3nm film on Si(100)

FIG. 4. Experimental Hf $4f$ photoelectron diffraction patterns exited with Mg $K\alpha$ for the 3 nm Hf film on Si(100) annealed at different temperatures. The percentage number in each pattern indicates its anisotropy (details in the text).

sample and due small misalignments of the transferable sample holder, the intensities of some regions in the diffraction pattern were slightly higher than others in the 360° azimuth scans (raw data). This effect was mainly observed in the high polar angles, typically at angles higher than 72°. To improve the visual quality, we have used a well-established fourfold average manipulation by expanding the data set in a Fourier series and extracting the components with fourfold symmetry. It is important to remark that this procedure did not introduce any diffraction peak or artifacts, it just corrected slightly the peak intensities and naturally removes the background, which has no defined symmetry. A detailed description is given in Ref. 20.

We would like to stress that other, essentially identical, samples annealed at a given temperature during 1 h produce XPD patterns similar to those for the consecutive annealed samples in Fig. 4. Several interesting conclusions can be derived from Fig. 4. The first is that HfSi$_x$ shows a clear transition from an amorphous or polycrystalline phase (for temperatures about 500 °C) at the surface/interface region to a crystalline phase (for higher annealing temperatures), which is in agreement with our XPS and LEED conclusions. For temperatures around 500 °C the diffraction pattern does not show an intensity variation, which is represented by the very low anisotropy and no periodic diffraction structures. For temperatures higher than 600 °C, the intensity variation in the diffraction pattern becomes visible, and periodic diffraction features are displayed. The low anisotropy in the diffraction patterns can be interpreted as a result from the short-range order structure formed first at the interface. As we consecutively anneal at even higher temperatures, the anisotropy increases, which indicates emission from a larger crystalline area, or better ordering of the sample or emitters deeper in the crystal. We should note that almost all the fine diffraction features displayed in the high temperature annealing patterns are already present in the sample annealed at 630 °C. Several experimental and theoretical studies[9–14] agree that the Hf silicide composition at high temperatures is in the form of HfSi$_2$. Thus, we assume, for the 3 nm Hf films investigated here, that once the Hf reacts with Si and forms an ordered phase, that phase is solely HfSi$_2$, and it is present in the interval from 600 to 1000 °C, as monitored by XPD experiments. That there are no additional features in the diffraction patterns, which would suggest another ordered structural phase, is a strong indication that only one ordered phase exists over the investigated temperature range. For example, if a monosilicide ordered phase existed at low temperatures, we would expect a different diffraction pattern (or at least some additional features) from that observed. This result appears to refute the possibility of a transition from one ordered phase to another when the annealing temperature is changed.[9,11–14]

Experimental XPD patterns by themselves rarely allow us to determine a structure nor do they exclude the possibility of the coexistence of multistructural phases. In order to answer this question, it is necessary to perform a systematic and comprehensive structural analysis of the XPD data through comparison of experiment and theoretical simulations.

In this paper, we present the results of preliminary calculations in order to test different structures. The theoretical simulations for the XPD patterns were performed by using the multiple scattering code as implemented in the MSCD package.[20] The calculations were performed with a parallel PC cluster using Pentium 4 processors running Linux RedHat 7.3 as the operating system. Because of the high electron kinetic energies for Hf $4f$ excited with Mg $K\alpha$ radiation the electron mean-free path is large, about 24 Å, and a multiple scattering approach was used in the simulations. Thus, large structure models are necessary to avoid cluster border effects in the simulations. In all the calculations, we

judiciously used six multiple scattering events and expansions up to the forth Rehr-Albers order.[20] The surface cluster was constructed with a semiparabolic shape, with a maximum radius and depth of 24 Å and 26 Å, respectively, corresponding to approximately 650 atoms. This choice of parameters permitted a compromise between the exactness of the calculations and the time and memory consumed to simulate a complete pattern; a single simulation for a whole diffraction pattern used about 1.2 Gbytes of RAM memory and 2-3 processing hours. In order to quantify the agreement between the experimental data and the theoretical simulations, we used the well established R_a-factor analysis.[20] The reliability factor used here is basically a normalized least-squares fit, where a lower R_a is interpreted as a better agreement between experiment and theory.

To test our theoretical approach, we simulated the Si 2*p* XPD pattern from the clean Si(100) surface and compared it with the experimental data set. For this simulation, most of the structural and nonstructural parameters were set to the tabulated bulk values, for example the band gap, and lattice parameter. The Debye temperature and surface inner potential were fitted to better adjust to the data set. The values thus determined were respectively 8.0 eV and 650 K, which are in good agreement to the tabulated values. The inclusion of twelve emitting layers was enough to simulate the pattern and further emitters did not improve significantly the R factor analysis. Because of the high electron kinetic energy in these experiments, the XPD pattern is almost insensitive to the fine structure, such as dimer reconstruction, on the clean Si(100) surface. This insensitivity allowed us to consider the unreconstructed surface as the model. The resulting experimental and theoretical patterns are presented in Figs. 5(a) and 5(b), respectively. For the clean surface [Fig. 5(a)] an excellent agreement to the simulated data [Fig. 5(b)] was obtained. This is also indicated by the good low R_a factor of 0.18. This result is an important reference because it represents a standard by which we evaluate the other models proposed for the $HfSi_2$.

In Fig. 5(c), we present the experimental Si 2_p XPD pattern from the $HfSi_2$ sample annealed at 945 °C. As was true for the LEED patterns, the XPD pattern is virtually identical to that for the clean Si sample, which supports the conclusion that $HfSi_x$ islands form, with large areas of clean Si(100). In this case, the Si 2_p signal from the $HfSi_2$ combines with that from the clean Si(100) surfaces and represents only a small contribution not distinguishable in this high energy pattern obtained from low resolution XPS spectra.

However, since the XPD patterns corresponding to the Hf 4*f* signal in Fig. 4 are quite different from that of Si in Fig. 5(a), it is clear that the Hf has a completely different crystallographic structure. Based on previous experimental and theoretical results from the literature,[10–13,22,23] we modeled the $HfSi_2$ crystal structural as $C11_b$ (MoSi₂ prototype), $C54$ (TiSi₂ prototype), or $C49$ (TiSi₂ and ZrSi₂ prototypes).

Figure 6 displays Hf 4*f* XPD patterns: the experiment corresponds to annealing at 945 °C and the simulated patterns correspond to the three different structural models. In the simulations reported here, we used tabulated bulk values for the structural parameters (i.e., $a=3.677$ Å, $b=14.550$ Å, and $c=3.649$ Å) and electronic parameters,[10–13,22] because
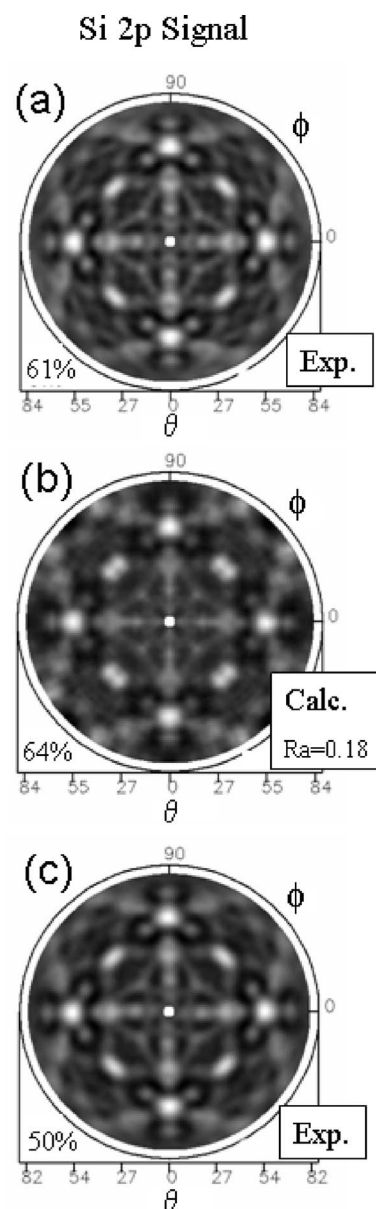

Si 2p Signal

FIG. 5. Experimental and theoretical Si 2*p* photoelectron diffraction patterns excited with Mg $K\alpha$. (a) Experiment from a clean Si (100) (2×1)-2D surface; (b) simulation for a clean Si(100) considering bulk parameters; and (c) experiment from the 3 nm Hf film on Si(100) annealed at 945 °C.

the Hf film was relatively thick. Since a search for the values of Debye temperature and inner potential did not improve significantly the simulation, they were assumed to be identical to the values founded for the clean Si surface, i.e, respectively 650 K and 8.0 eV. Due the large unit cells of the $HfSi_x$ a maximum of five Hf emitters have been used in all the simulated patterns. From the R_a factor and from a visual comparison, it is clear that $C49$ is the structure that best describes the experimental data, in agreement with other work[10] that suggests the $C49$ structure to be the most stable one for $HfSi_2$. For a very similar system, that of $TiSi_2$, several reports[23] indicate the possibility of a phase transition between the $C54$ to the $C49$ structures and of the coexistence of both structures. In order to verify this possibility, we com-
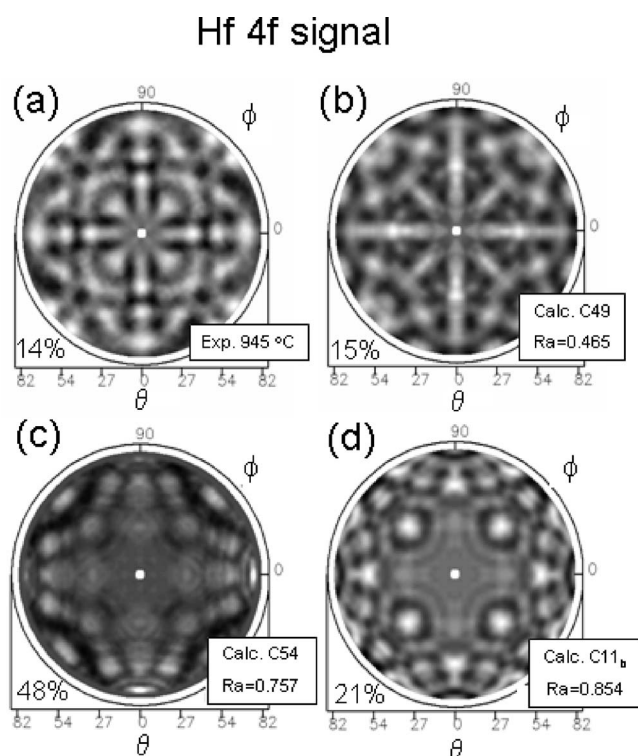
Hf 4f signal

FIG. 6. Experiment-theory comparison for the Hf $4f$ photoelectron diffraction patterns in an $HfSi_2$ for different crystal structures models. (a) shows the experimental pattern (film annealed at 945 °C), and the simulated patterns are present in (b) for the $C49$ structure, (c) for the $C54$ structure, and (d) for the $C11_b$ (details in the text).

FIG. 7. Example of cluster model for the $C49$ structure with bulk parameters and terminated in Si-Si layers.

bined the different simulated patterns in Fig. 6 statistically. All attempts led to R_a factors that were higher than that obtained for pure $C49$ which indicates that for our annealing temperature $HfSi_2$ has only one crystallographic phase, the $C49$.

Although the R_a factor of 0.465 for the $C49$ pattern in Fig. 6(b) is much lower than those for the other structures studied, which are unacceptable, it is still higher than the R_a factor for a good simulation, such as that for clean Si in Fig. 5 (i.e., $R_a = 0.181$). But, despite the elevated global R_a factor for the $C49$ structure in Fig. 6(b), when we analyze the azimuthal spectra for each polar angle separately, we discover that most individual R_a factors are lower than 0.25: the global value is higher because some of the azimuthal spectra are poorly described by the $C49$ model with bulk parameters. We feel that the present results adequately distinguish the $C49$ structure as the best model of the $HfSi_2$ structure, but recognize that a study incorporating full relaxation of the structure is necessary for a definite resolution of the $HfSi_2$ structure.

In order to appreciate the importance of full relaxation, we should provide some details about the structure at this point. The Si(100) surface manifests a square shape, while $HfSi_2$ is rectangular in the $C49$ configuration. When the $HfSi_2$ grows on the Si(100) surface, it forms two sets of orthogonal islands: in one, the [010] direction of HfSi2 is parallel to the [001] direction of Si and, in the other, the [100] direction $HfSi_2$ is parallel to the Si [110] and [1−10]
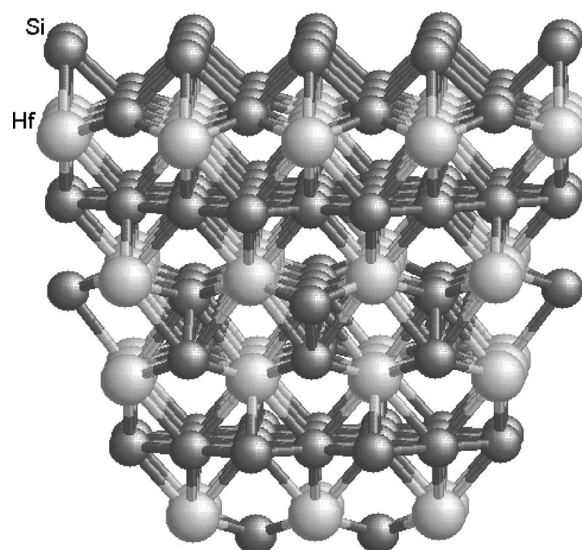
directions. In the surface plane, the lattice parameter mismatch is −4.3% in one direction and −5.0% in the other, so that we expect that the interface and at least the first few atomic layers of the $HfSi_2$ to be distorted from the bulk values by expansions and contractions. In Fig. 7 we present a cluster model of the $C49$ structure used in the simulations. For this reason, it is probable that the angular positions of some strong diffracting features in the simulated patterns we present in Fig. 6 deviate from the correct values. Given our high energy data set, our computational approach and facilities, and the fact that correct resolution of this complicated structure requires optimization of several parameters, which is an extremely lengthy computational chore, complete relaxation of this structure was not possible in the present study. We are planning a new study where new search algorithms will be applied for solving the structure using simultaneously the present high energy data and a more surface sensitive data set taken with low energy and high resolution synchrotron radiation.[21]

B. Ultra thin Hf films (<0.3 nm)

For the thick Hf film we have considered so far, there was no evidence of ordering at low temperatures. In order to eliminate the possibility that the lack of ordering is related to the film thickness, we consider here ultrathin Hf films, where the behavior of the silicide formation could be strongly affected by the Si substrate. The possibility of multiple phases at different temperatures also exists. To investigate these possibilities we prepared an approximately 0.3 nm thick Hf film using the same method as described in Sec. II, which we study with the same procedure as that used for the thick film.

For the sample as evaporated at RT, the LEED exhibited no diffraction pattern. When we anneal at 550 °C, a $p(1 \times 1)$) pattern appears, with weak (2×1) spots; for 580 °C annealing, the (2×1)) pattern appears clearly, but with some diffuse background; and for annealing temperatures higher
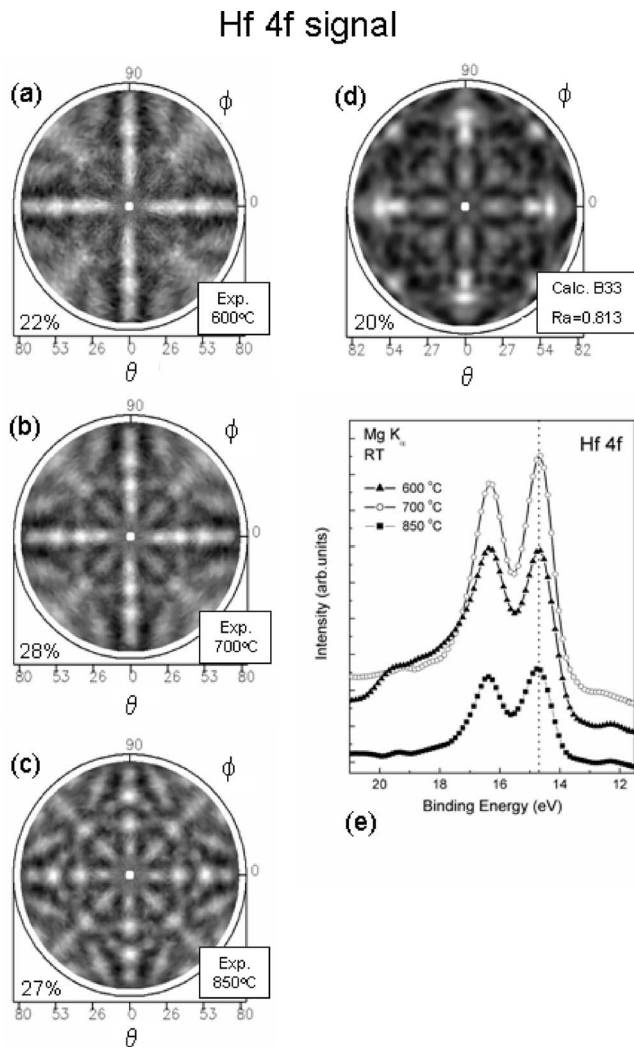
Hf 4f signal

FIG. 8. XPD and XPS results for an ultrathin Hf film evaporated on Si(100) and annealed at different temperatures. Experimental XPD patterns are shown in (a), (b), and (c) respectively to the film annealed at 600, 700, and 850 °C. In (d) is shown a simulated XPD pattern considering an HfSi in the $B33$ crystallographic structure [the R_a factor is related to the comparison with the pattern (a)]. (e) XPS spectra for the Hf 4f after sample annealing at different temperatures.

then 600 °C) the LEED pattern is the same as that for the clean Si(100) surface. We again interpret the data as corresponding to a homogeneous film at low temperatures with nucleation of islands for high annealing temperatures.

In Figs. 8(a)–8(c), we present experimental Hf 4f XPD patterns for the ultrathin film for annealing temperatures of 600 °C, 700 °C, and 850 °C, respectively; Fig. 8(d) corresponds to a theoretical simulation which we discuss below; and Fig. 8(e) represents the corresponding Hf 4f XPS spectra. The Hf 4f peaks show no appreciable shifts in the silicide components upon annealing. However, for 600 °C annealing, the peaks are more asymmetric, which could indicate an additional component at higher binding energies: we should note that such a component would not necessarily be a silicide, but could be a silicate.[24] In fact, it is possible to see a clear contribution of one HfO_x component in the spec-

trum at values around 19.7 eV binding energy. It most probably originates from a small O_2 contamination during the evaporation process and from Hf reacting with oxygen present in the sample holder. For the peak position, again it is not possible to identify a large shift upon successive annealing temperatures.

The experimental XPD patterns for this sample show different features when compared to those for the 3 nm film. In order to study the possibility of HfSi formation, we present, in Fig. 8(d), a simulation using the $B33$ structure (CrB prototype) which is indicated to be one of the possible crystalline structures of HfSi.[11,15] It is clear, from Fig. 8(d), that such a structure does not represent the data [the R_a factor displayed in the figure is for the comparison with the data set of Fig. 8(a)]. We believe that the $HfSi_x$ forms as a disilicide, in the same $C49$ structure as for the thick film, however, with most probably Hf emitters diffusing only into the first few layers and with its lattice parameter highly distorted from the tabulated bulk value.

The difference in the XPD patterns for low coverage compared with the high coverage probably results from of the absence of the contributions of subsurface Hf emitters to the diffraction peaks and probably because of the different structural parameters produced by strong interaction with the silicon substrate. A detailed structural determination for this lower coverage, including synchrotron radiation measurements, is highly desirable.

Despite the results found in the previous section for the thick Hf film, it would be interesting to present a careful analysis between the experimental patterns shown in Fig. 4 (600, 630, 945, and 1012 °C) and the models for the disilicide phase ($C49$) and monosilicide phase ($B33$). Looking to the low polar angles it seems that the B33 model shown in Fig. 8(d) better compares with the experimental data sets for the thicker films [for example that one presented in Fig. 4(a)]. However, definitely it is not the case for the high polar angles which has a good comparison with the $C49$ model. The question that immediately appears is that the data sets might be interpreted by a linear combination of these two models, which would turn out to be a strong indication of phase coexistence. In Fig. 9(a) is presented the R_a factor analysis as function of the linear combination of the two models (0% of $C49$ phase means a pure $B33$ model). The heavy black curve shows the R_a factor averaged over all polar angles (i.e., considering the whole data set). It is clear that the best value is for a pure $C49$ structure. Looking for some particular polar angles is evident that high concentrations of the $B33$ model only produce good R_a factor for polar angles lower than 8°, which is a region without too much structural information. The absence of a minimum in the R factor curves though the different concentrations suggest that the combination is not the true model. These results show that most probably the $HfSi_2$ film is crystallized in a very distorted $C49$ structure where the correct packing and distances for the first layers are between the $B33$ and the $C49$, which is also indicated by the not complete agreement in the position of the diffraction peaks as can be observed in the patterns and in the detailed polar scan showed in Fig. 9(b).
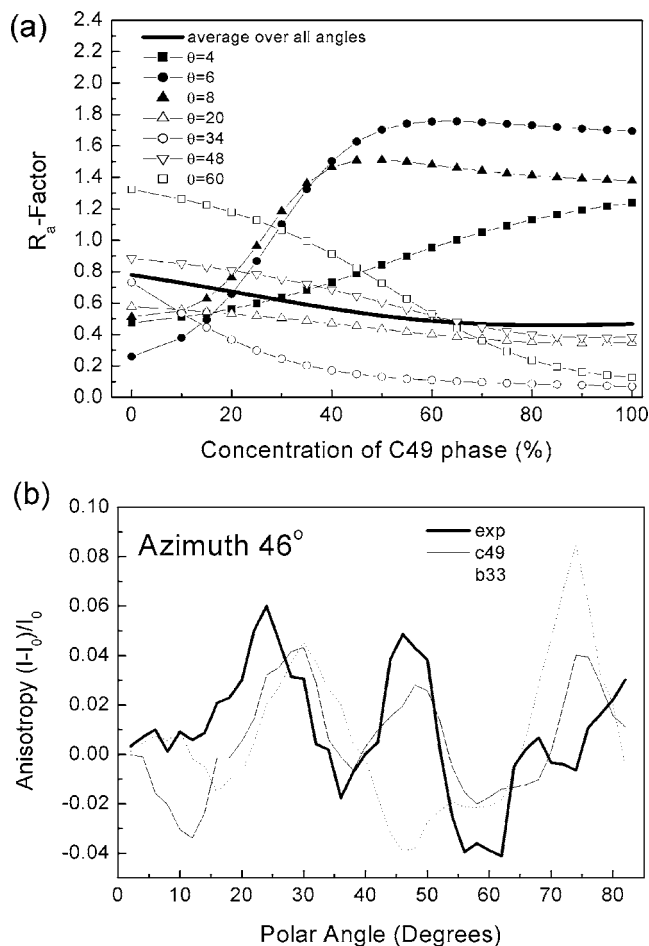
FIG. 9. (a) R_a factor analysis for the linear combination of HiSi$_2$ (C49) and HfSi (B33) models (details in the text). (b) Polar curves at azimuth angle equal 46°. Comparison between the high coverage Hf-silicide film (film annealed at 945 °C) (heavy curve) and two theoretical models C49 (light curve) and B33 (dot curve).

IV. CONCLUSIONS

The present work represents the first photoelectron diffraction study of Hf silicide interface formation on the Si(100) surface. We carried out a systematic investigation of the surface crystalline structure formation upon consecutive annealing temperatures in different thickness limits of metallic Hf evaporated onto clean Si(100)-(2×1)-2D surfaces.

XPS clearly indicates that hafnium silicide starts to appear on the clean Si surface at annealing temperatures as low as 300 °C. For annealing temperatures around 500 °C, almost all the metallic Hf is converted to at least one silicide component and forms an amorphous or polycrystalline phase. For annealing at 550–600 °C, the low anisotropy XPD pattern presented in Fig. 4 corresponds to a short range order crystalline contribution from the HfSi$_x$/Si interface, which is in a good agreement with the results obtained for the ultrathin film. The combination of LEED and XPD analysis of the Si 2_p signal permit us to conclude that 3D islands form, especially in the high temperature annealing regime. These findings are in agreement with previous AFM and STM results.[14,17,18] The most important conclusion presented in this paper, which requires the unique characteristics of XPD experiments, is that we found no experimental evidence for a structural phase transition from an ordered HfSi to an ordered HfSi$_2$ as the sample is annealed. We propose only one structural phase as a result of an annealing in the temperature range from 600 °C to 1000 °C. In the literature, only very few studies,[11–14] most of them are based on XPS results only, report a monosilicide phase in this temperature regime. Since other experiments, for example, x-ray diffraction, using other, perhaps thicker, films prepared in other ways than in UHV, might reach different conclusions, we hope that this paper would motivate other investigations in this direction.

We performed a preliminary structural determination by testing different crystal structure models for HfSi$_2$ and HfSi, using their bulk structural and electronic parameters tabulated in the literature. The best theory-experiment comparison indicates that the HfSi$_2$ is present in the C49 structure for the 3 nm Hf film. Because of the computational complexity and the time consumed in the simulations of high-energy photoelectron diffraction patterns, we did not try to refine the C49 structure. We are planning a further experiment, where low energy and high resolution photoelectron diffraction data obtained with synchrotron radiation will allow better refinement in the structure analysis.

*Corresponding author. Email address: abner@lnls.br

[1] G. E. Moore, Electronics **38**, 8 (1965).

[2] G. D. Wilk, R. M. Wallace, and J. M. Anthony, J. Appl. Phys. **89**, 5243 (2001).

[3] Clemens J. Först, Christopher R. Ashman, Karlheinz Schwarz, and Peter E. Blöchl, Nature (London) **427**, 53 (2004);, and references therein.

[4] B. Cheng, M. Cao, R. Rao, A. Inain, P. V. Voorde, W. M. Greene, J. M. C. Stork, Z. Yu, P. M. Zeitzoff, and J. C. S. Woo, IEEE

Trans. Electron Devices **46**, 1537 (1999).

[5] T. J. Hubbard and D. G. Schlom, J. Mater. Res. **11**, 2757 (1996).

[6] B. H. Lee, L. Kang, Renee Nieh, Wen-Jie Qi, and Jack C. Lee, Appl. Phys. Lett. **76**, 1926 (2000).

[7] S. Toyoda, J. Okabayashi, H. Kumigashira, M. Oshima, K. Ono, M. Niwa, K. Usuda, and G. L. Liu, Appl. Phys. Lett. **84**, 2328 (2004); Appl. Surf. Sci. **216**, 228 (2003); J. Electron Spectrosc. Relat. Phenom. **144-147**, 487 (2005).

[8] S. Suzer, S. Sayan, M. M. Banazak Holl, E. Garfunkel, Z. Hus-

sain, and N. M. Hamdan, J. Vac. Sci. Technol. A **21**, 106 (2003).

[9] C. J. Kircher, J. W. Mayer, K. N. Tu, and J. F. Ziegler, Appl. Phys. Lett. **22**, 81 (1973).

[10] G. Shao, Acta Mater. **53**, 3729 (2005).

[11] W. Y. Hseih and L. J. Chen, J. Appl. Phys. **76**, 278 (1994).

[12] C. S. Chang, C. W. Nieh, and L. J. Chen, J. Appl. Phys. **61**, 2393 (1987).

[13] J. F. Smith and D. M. Bailey, Acta Crystallogr. **10**, 341 (1957).

[14] H. T. Johnson-Steigelman, A. V. Brinck, S. S. Parihar, and P. F. Lyman, Phys. Rev. B **69**, 235322 (2004).

[15] A. Raman and H. Steinfink, Acta Crystallogr. **22**, 688 (1967).

[16] S. Tanuma, C. J. Powell, and D. R. Penn, Surf. Interface Anal. **21**, 165 (1993). The IMFP have been calculated using the QUASES-IMFP code.

[17] J.-H. Lee, J. Korean Phys. Soc. **44**, 1590 (2004); Appl. Surf. Sci. **239**, 268 (2005).

[18] J.-H. Lee, and M. Ichikawa, J. Vac. Sci. Technol. A **20**, 1824 (2002).

[19] N. Miyata, Y. Morita, T. Horikawa, T. Nabatame, M. Ichikawa, and A. Toriumi, Phys. Rev. B **71**, 233302 (2005).

[20] Y. Chen and M. A. Van Hove, http://electron.lbl.gov/mscdpackage.htm

[21] C. Flüchter, D. Weier, A. de Siervo, M. Schürmann, S. Dreiner, M. F. Carazzolle, R. Landers, G. G. Kleiman, and C. Westphal (unpublished).

[22] *Pearson's Handbook of Crystallographic Data for Intermetallic Phases*, 2nd edition, edited by P. Villars and L. D. Calvert (Materials Park, OH: ASM International, 1991).

[23] M. Iannuzzi, P. Raiteri, M. Celino, and L. Miglio, J. Phys.: Condens. Matter **14**, 9535 (2002) and ref. therein.

[24] J.-H. Lee, Thin Solid Films **472**, 317 (2005).